Microstructural Behaviors of Polyaniline/CB Composites by SAXS

Siddaramaiah,[1,2] Fernando G. Souza Jr.,[2] Bluma G. Soares,[2] P. Parameswara,[3] R. Somashekar[3]

[1]*Department of Polymer Science and Technology, Sri Jayachamarajendra College of Engineering, Mysore 570006, India*
[2]*Institute of Macromolecules, Centro de Tecnologia, Federal University of Rio de Janeiro, Bl J, Ilha do Fundão, Rio de Janeiro, RJ 21945-970, Brazil*
[3]*Department of Studies in Physics, University of Mysore, Manasagangotri, Mysore 570006, India*

Received 10 March 2009; accepted 2 June 2009
DOI 10.1002/app.30904
Published online 10 December 2009 in Wiley InterScience (www.interscience.wiley.com).

ABSTRACT: Polyaniline doped with dodecylbenzene sulfonic acid and conductive carbon black (PAn.DBSA/CB) hybrid materials have been prepared by *in situ* polymerization. The electrical resistivity of the PAn/CB was measured as a function of CB. The minimum resistivity was noticed for the composites with 25 wt % of CB as compared to other systems. Small angle x-ray diffraction data was used to characterize the molecular arrangements of these composites. The refinement parameters such as periodicity (L), phase lengths ($<Y>$ and $<Z>$), phase ratio ($<Y>/<Z>$), and probability distribution of phases [γ_Z (crystalline), γ_Y (amorphous)] for PAn, CB, and PAn/CB composites have been measured by SAXS data. It was observed that there is decrease in the crystallinity with increase in CB content in the composites.
 J Appl Polym Sci 116: 673–679, 2010

Key words: carbon black; polyaniline; hybrid material; conductivity; microstructural parameters

INTRODUCTION

Ever since the discovery of inherently conducting polymers (ICPs), research dealing with the applications of these unique materials continues to grow. When these ICPs are combined with other conducting materials, some unique properties can be produced. They have extensively used in electrochromic displays,[1] electronic devices,[2] chemical sensors,[3,4] etc. The use of ICPs, especially polyaniline (PAn) and polypyrrole (PPy), and carbon black (CB) as conductive additives in the thermoplastic industries are limited due to undesirable properties of each at high temperatures. Carbon black-ICP composites, however, have shown improved performance at higher temperatures.[5]

Among the conducting polymers, PAn has attracted renewed interest from recent researchers as it is highly conducting and easy to synthesize both chemically (in powder form) and electrochemically (as a film). It is cheap and stable to heat and atmosphere. It is also the first conducting polymer available commercially.[6]

The development of composites constituted by conducting polymers with other conducting materials is also very important to combine the specific properties of each component. Del Rio et al.[7] have first reported the electrochemical synthesis of PAn/CB composites in a solution containing aniline and carbon black suspension. Before this, similar operation for the synthesis of polypyrrole and CB composites had been reported.[8]

Polyaniline conducting composites with CB,[9–11] graphite,[12,13] metal powders,[14] and carbon nanotubes (CNTs)[15–19] are routes to improve effectively the electrical and thermal conductivity. Among them, the low cost PAn/CB composites are expected to have potential applications in detection discrimination of amines,[20] novel rubbers,[21] and rechargeable batteries.[22] The composites of PAn with other conducting fillers are more stable than pure PAn and result in easy processability with thermoplastics.

The hybrid conducting composite materials have been prepared by *in situ* polymerization of aniline in the presence of Printex XE2B CB using dodecyl benzene sulfonic acid (DBSA) as the protonating agent and ammonium persulfate as the oxidizing agent.[11] The use of DBSA is very interesting because of the better processibility and compatibility that can be achieved when these materials are used in blends with insulating polymers. In this article, authors

Correspondence to: Siddaramaiah.
Contract grant sponsors: Conselho Nacional de Desenvolvimento Científico e Tecnológico (CNPq), Fundação de Amparo à Pesquisa do Estado do Rio de Janeiro-FAPERJ, Petroflex S.A.

reported the microcrystalline behavior of PAn protonated with dodecyl benzene sulfonic acid (DBSA). It is surprising that, there is a Bragg like reflection at q ($= 4\pi\sin\theta/\lambda$) = 0.007/Å, which gives a long periodicity of 930 Å. Such long periodicity is only observed in natural materials like collagen.[23] Taking this as a Bragg like reflection, we have carried out the profile analysis on the basis of Hosemann's two phase model.

EXPERIMENTAL

Materials

Carbon black (CB; printex XE-2, DBP = 370 mL/100 g, BET = 1000 m^2/g, density = 2.04–2.11 g/cm^3) was kindly supplied by Degussa (Frankfurt, Germany). Aniline (analytical grade from Vetec, Brazil), ammonium peroxydisulfate (APS) (analytical grade from Vetec, Brazil) and DBSA (commercial grade from Solquim LTDA, Brazil) were used without further purification.

Synthesis of PAniDBSA and the hybrid materials

Polyaniline doped with DBSA (PAn.DBSA) and their composites with carbon black (CB) were synthesized by one step route in toluene medium. In a typical procedure, 4.7 mL (0.051 mol) of aniline and 16.7 g (0.051 mol) of DBSA were dissolved in 250 mL of toluene under constant stirring. The medium was kept at 0°C and an aqueous solution containing 11.36 g (0.051 mol) of APS in 40 mL of water was slowly added over a period of 20 min. After 6 h, the reaction medium was poured into methanol, filtered, washed several times with methanol, and dried. In the case of PAn.DBSA–CB composites (PAn.DBSA/CB) different amounts of CB were first dispersed in toluene. After the polymerization, the emulsion of PAn.DBSA/CB was precipitated in methanol. The dark green precipitate was filtered, washed several times with methanol, and finally vacuum dried for 24 h. The conversion of aniline into polymer was determined gravimetrically from the difference between the total weight of sample obtained in the experiment and the weight of CB initially present in the medium. Assuming that the formed PAn contains 50% of the nitrogen in the imine form, all imine groups were protonated by the DBSA.

Characterization

The electrical resistivity measurements of PAn.DBSA, CB, and PAn.DBSA/CB were performed by the conventional four probe method, as per the procedure reported elsewhere.[24] The equipment used for this measurements is composed by an electrometer Keithley 6517A, a multimeter Minipa ET2907 and a home made four probes device with a minimum distance between the probes of 0.171 ± 0.03 cm. The specimens for surface resistivity measurements were pressed into disks of 38 mm diameter and about 1 mm thickness using hydraulic press for 5 min.

Small angle X-ray scattering

Small X-ray scattering (SAXS) measurements were performed using the beam line of the Brazilian's Synchrotron Light Laboratory (LNLS—Brazil; D11A-SAXS1 #5324/06; D11A-SAXS1-7086/08). This beam line is equipped with an asymmetrically cut and bent silicon (111) monochromator (λ = 1.488Å), which yields a horizontally focused X-ray beam. A linear position sensitive X-ray detector (PSD) and a multichannel analyzer were used to determine the SAXS intensity, $I(q)$, as function of the modulus of the scattering vector $q = (4\pi/\lambda)\sin\theta$, θ being the scattering angle. All SAXS spectra were corrected for the parasitic scattering intensity produced by the collimating slits, for the non-constant sensitivity of the PSD, for the time varying intensity of the direct synchrotron beam and for differences in sample thickness. Thus, the SAXS intensity was determined for all samples in the same arbitrary units, so that they can be directly compared. Since the incident beam cross-section at the detection plane is small, no mathematical desmearing of the experimental SAXS function was needed.

Theory of SAXS

The linear paracrystalline model of polymer morphology comprises of stacks containing a finite number of crystalline lamellae separated by amorphous segments. The thickness of successive lamellae along a stack is randomly selected from a certain probability density function, as the length of amorphous segment, although they may be distributed according to a different function. If it is assumed that the transverse width of a stack is infinite and that the lamellae boundaries are flat and normal to the axis, then the X-ray beam normal to stack axis will be scattered along a line in reciprocal space parallel to the stack axis on the distribution of intensity along this will be given at small angles. The equation is given by[25]:

$$\frac{2I(\pi S)^2}{\Delta\rho^2} = Re\left[\frac{(1-H_Y)}{(1-H_YJ_Z)}\left\{N(1-J_Z) + \frac{J_Z(1-H_Y)(1-H_YJ_Z)^N}{(1-H_YJ_Z)}\right\}\right] \quad (1)$$

TABLE I
Resistivity and Composition of PAn.DBSA/CB Hybrid Materials

Components weight (g)			Composition of the composite		
Aniline	CB	Conversion of PAn.DBSA (wt %)	PAn.DBSA (wt %)	CB (wt %)	Resistivity (Ω cm)
4.76	0.00	49	100	0	8.70E + 00
4.79	1.60	46	75	25	1.11E + 00
4.83	4.46	72	52	48	2.94E + 02
0.0	5.40	–	0	100	1.28E + 00

where, H_Y and J_Z are, respectively, the Fourier transforms of the normalized distribution function of lengths Y and Z of the amorphous and crystalline phase segments, $S(=4\pi\sin\theta/\lambda)$ is the scattering vector, 2θ is the scattering angle, and λ is the wavelength of radiation $N(=20$ units) is the number of repeating units in a stack, $\Delta\rho$ is the difference between the electron densities of the phases and $I(s)$ is the scattering intensity as a function of scattering angle parallel to stack axis. If it is assumed that the fiber comprises of parallel stacks, incoherently arranged, there will be distribution of intensity scattered by fiber. A correction of broadening of intensity profile has been reported[26] and incorporated here.

Using exponential distributions for H_Y and J_Z, Hosemann's eq. (1) is expressed in a form which is amenable to computational analysis and is given by:

$$\frac{2I(\pi S)^2}{\Delta\rho^2} = \frac{C}{F} + \frac{(D+E)}{F^2} \tag{2}$$

where,

$$F = 1 + A^2B^2 - 2AB\cos X \tag{3}$$

$$C = N\{1 - A^2B^2 - A(1-B^2)\cos\phi - B(1-A^2)\cos\chi\} \tag{4}$$

$$D = \frac{B[(1-A^2)(1-A^2B^2)\sin X\sin\phi + \{(1+A^2B^2)\cos X - 2AB\}\{(1+A^2)\cos\phi - 2A\}]}{G} \tag{5}$$

$$G = 1 - A^NB^N\cos NX \tag{6}$$

$$E = A^NB^{N+1}\sin NX[(1-A^2B^2)\{(1+A^2)\cos\phi - 2A\} \times \sin X - (1-A^2)\times\{(1+A^2B^2)\cos X - 2AB\}\sin\phi] \tag{7}$$

For given values of A, B, χ, and ϕ, $I(S)$ can be evaluated from the eqs. (2)–(7). A, B, χ, and ϕ are the values of Fourier transforms of the probability distributions of the amorphous and crystalline phase lengths. A and χ are related to the distribution of phase-Y segment lengths and B and ϕ to that of phase-Z segment lengths.[27]

Scanning electron microscopy

The morphology of the samples was measured by scanning electron microscopy (SEM) on a JEOL equipment model JSM 5300 with 10 kV of voltage acceleration. All samples were coated with thin layer of gold and microphotographs were recorded.

RESULTS AND DISCUSSION

Electrical resistivity of the hybrid materials

The effect of the CB content on the conversion of aniline into PAn.DBSA and electrical resistivity of the hybrid composites have been studied and obtained values are given in Table I. The degree of conversion of PAn.DBSA at low CB loading level is low. However, at higher amount of CB, the conversion of PAn is substantially high. This may be due to the ability of the CB in adsorbing DBSA molecules, thus making difficult the complete elimination of the acid during the washing process.

The electrical resistivity of PAn.DBSA/CB composites also depends upon the amount of CB in the composite. At lower CB loads (25 wt %); the minimum values of resistivity was noticed. This result indicates that, CB particles act as electrically

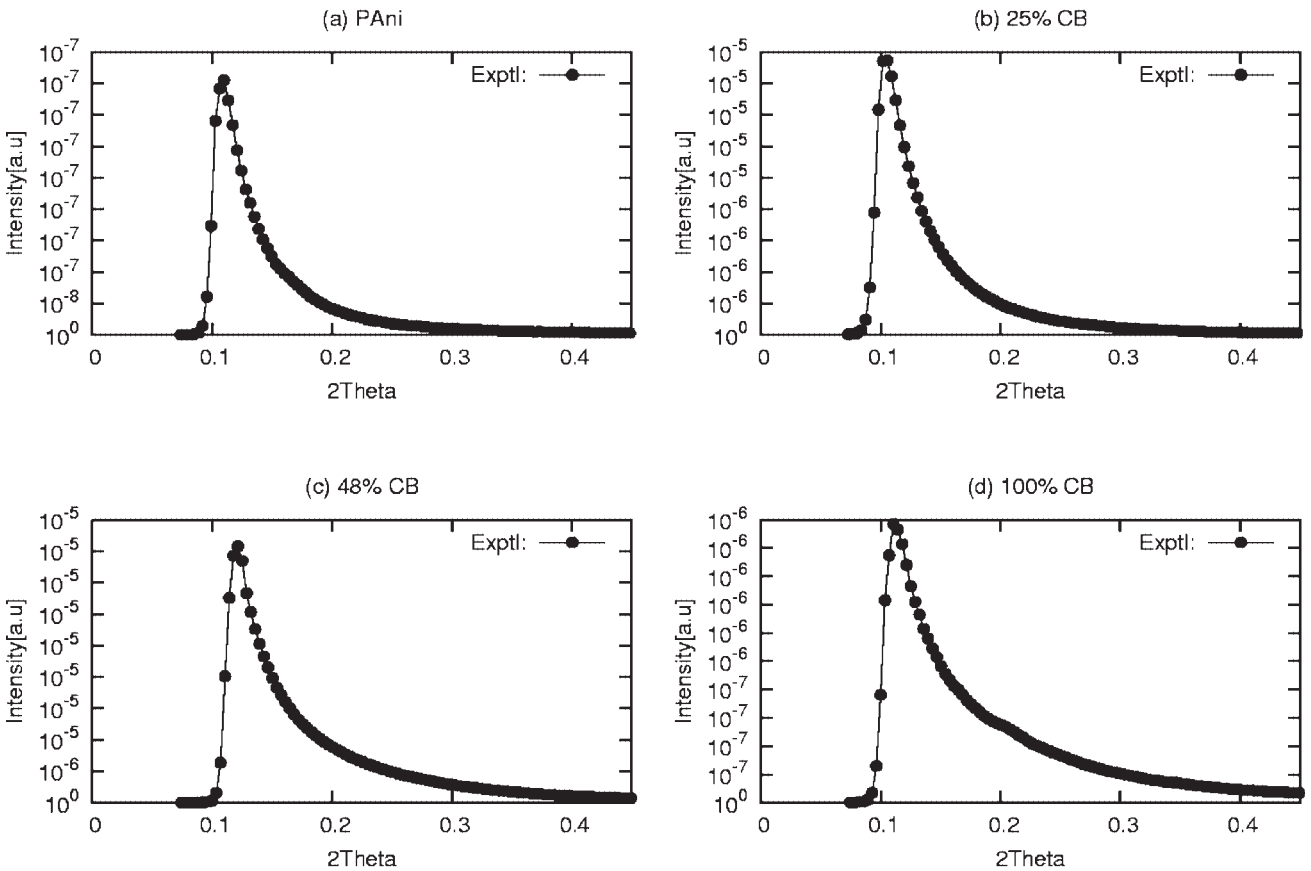

Figure 1 SAXS data profiles for pure sample and different concentration of CB; (a) PAn, (b) 25% CB, (c) 48% CB, and (d) 100% CB.

conductive bridges. Similar behavior has been also reported for composite constituted by PAn and graphite.[28] After this point, there is an increase of resistivity, whose values are slightly higher as compared to pure systems.

Microstructural parameters

Figure 1 shows the small angle x-ray diffraction patterns of the PAn.DBSA, CB, and PAn.DBSA/CB composite. The structure of the crystalline phases of PAn.DBSA is orthorhombic.[29–31] Using eqs. (1)–(7) and SAXS data, the microcrystalline parameters have been computed for all the samples. For this purpose we have written a refinement program which simulates SAXS profile with refinement parameters like periodicity (L), phase lengths ($\langle Y \rangle$ and $\langle Z \rangle$), phase ratio ($\langle Y \rangle / \langle Z \rangle$), number of repeat unit in the stack (N), crystallinity, and probability distribution of phases γ_Z (crystalline), γ_Y (amorphous) for different concentration of PAn.DBSA/CB and the values obtained after several refinement with good convergence, are given in the Table II.

The increase in CB content in composite resulted in different SAXS patterns with peaks of lower intensity, indicating a decrease in percentage of crystallinity region. Sharp peaks in pristine sample become weak and broad as the concentration of CB in the composite increases. This indicates that the

TABLE II
Microstructural Parameters of PAn.DBSA/CB Hybrid Materials Obtained Using SAXS

Sample	PAn.DBSA (wt %)	CB (wt %)	Periodicity in Å	Phase ratio	γ_Y	γ_z	$\langle Y \rangle$ in Å	$\langle Z \rangle$ in Å	N	Crystallinity $\frac{\langle Z \rangle}{\langle Y \rangle + \langle Z \rangle}$
PAn	100	0	828.38	0.0062	0.604	0.001	5.12	823.26	10	0.99
PXE (25%)	75	25	930.74	0.0156	0.001	0.011	14.52	916.22	15	0.98
PXE (48%)	52	48	892.15	0.0936	0.153	0.027	83.50	809.00	12	0.90
CB	0	100	903.44	0.1	0.197	0.030	90.34	813.10	10	0.90

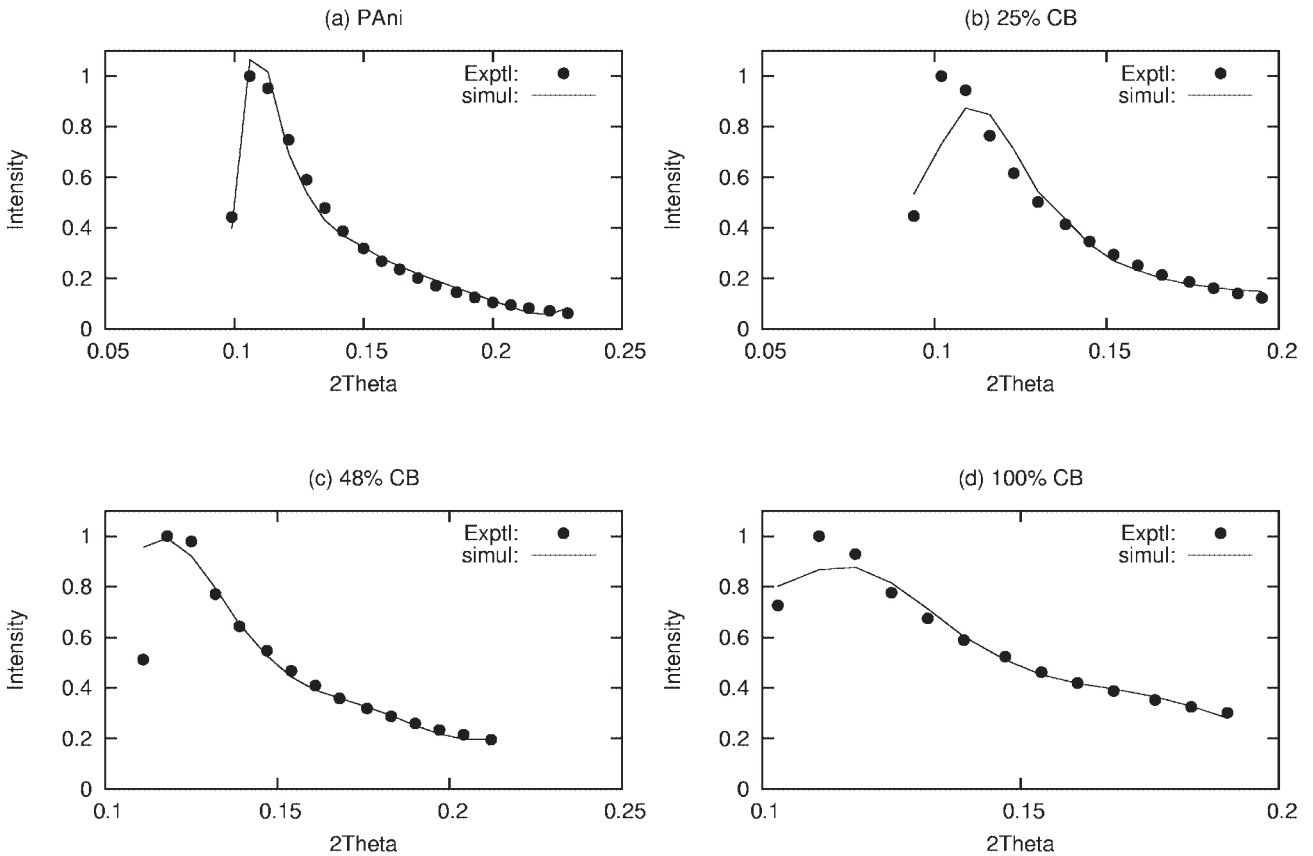

Figure 2 Simulated and experimental intensity curves using SAXS profiles and employing the model parameters; (a) PAn, (b) 25% CB, (c) 48% CB, and (d) 100% CB.

presence of CB in a high proportion disturbs the crystallization region of the PAn chains. The PAn.DBSA/CB composite with 48 wt % of CB showed amorphous pattern similar to pure CB. This may be due to the high CB content as acted as thread "impurities" to the growth of the PAn crystallites, which results in formation of amorphous PAn.

Figure 2 shows simulated and experimental intensity curves using SAXS profiles and employing model parameters. Here, model parameters are periodicity of the stacks, length of the amorphous segment, length of the crystalline segment and width of the distribution. It is evident from Table II that, there is an increase in the periodicity, phase ratio and phase length of amorphous region with increase in CB content. The probability distribution function of crystalline length for pure sample is too low, which increases with concentration of CB. The composite containing 25 wt % CB exhibits significantly high value of periodicity and probability distribution of crystalline length. High value of periodicity indicates the crystalline like order in polymer network extends to a large segment, compared to amorphous region. Stacking of crystalline regions is separated by amorphous segments. In PAn, amorphous segment is only 0.6% of the total long range ordering. With the addition of CB (25 wt %), this amorphous segment increases slightly to 1.6% associated with increase in crystalline segment from 823 Å to 916 Å. This slight increase in amorphous segment reduces overall crystalline long range order only marginally. Further increase in CB is associated with increase in amorphous region and hence therein appreciable decrease in the long range crystalline order. A schematic representation of two phase paracrystalline model (for SAXS and WAXS) is shown in Figure 3.

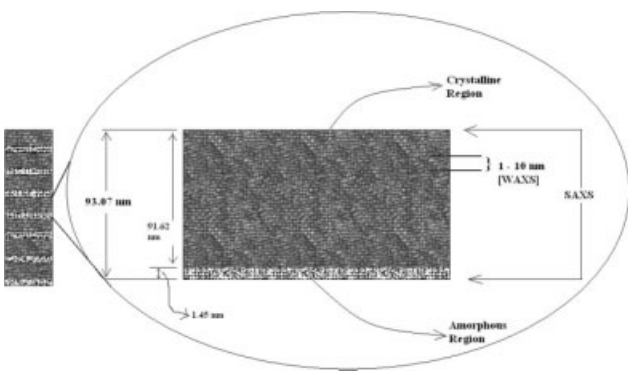

Figure 3 Two phase paracrystalline model (not drawn to scale).

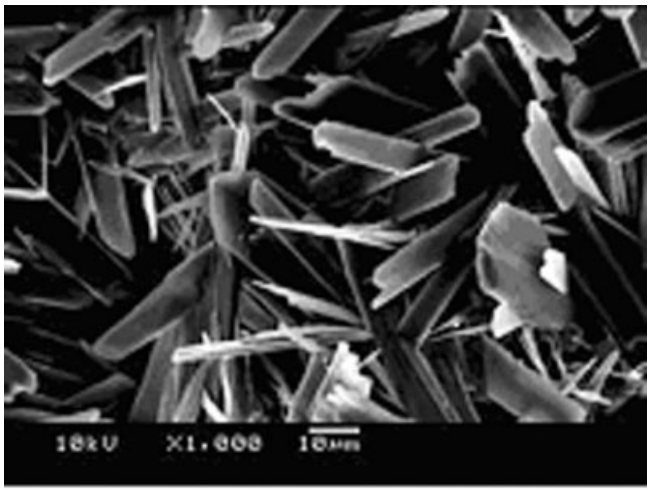

(a)

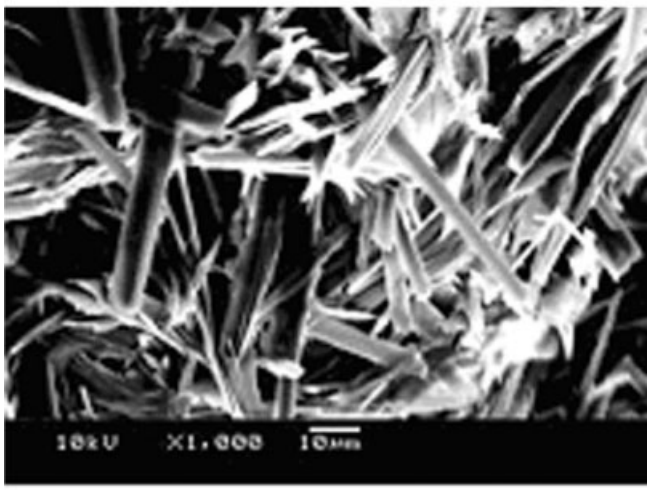

(b)

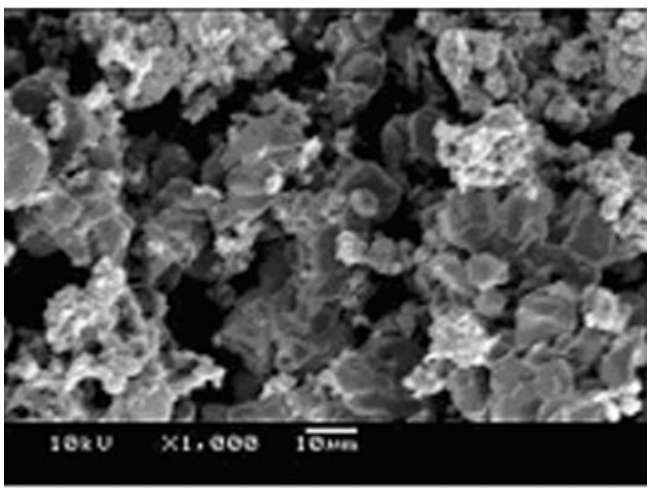

(c)

Figure 4 SEM photomicrographs of PAn/CB composites; (a) PAn, (b) 25% CB, and (c) 48% CB.

The resistivity data reveals that, the composite with 25 wt % of CB, which presents the lowest resistivity and also a tubular morphology, does not show sharper peaks in x-ray diffraction, suggesting that the most important feature to achieve higher conductivity is the formation of microtubular morphology.[11] These results evidently emphasis that with greater ordered entangled polymer network with a periodicity of the order 1000 Å results in a good resistivity material. It should be emphasized here that, the crystalline like order with a periodicity in the range 10–100 Å (WAXS) may have entirely different features compared to the crystalline like order in the periodicity of range 1000 Å (SAXS). We have integrated the connection between physical measurements in terms of long range crystalline like order with periodicity of 1000 Å.

Figure 4(a–c) shows the SEM images of the PAn.DBSA and PAn.DBSA/CB composites. Figure 4(a) indicates the fiber structure for PAn. SEM images of PAn with lower content of CB (25%) also indicate the fiber structure, whereas higher CB content systems showed domains (spherical shape) of PAn/CB composites. The SEM photographs clearly indicates that the morphology with the composition of the composites and presence of physical interaction between PAn and CB.

CONCLUSIONS

PAn.DBSA/CB hybrid materials were synthesized by *in situ* polymerization. The presence of low amount of CB (up to 25 wt %) resulted in a decrease in resistivity as compared to pure PAn.DBSA. The composite containing 25 wt % CB also displayed a tubular morphology characterized by microtubules with high aspect ratio. Higher amount of CB give rise to materials with higher resistivity values similar to pure carbon black. Surprisingly, the composite containing 25% of CB, which displayed the lowest resistivity value, also presented a decrease in crystallinity. Further, there is a maximum associated with the crystalline phase lengths, phase ratio, and periodicity with the composite containing 25% of CB inconformity with the other physical measurements. At this CB concentration, the decrease in crystallinity and protonation degree do not exert substantial influence on resistivity.

The author (Prof. Siddaramaiah) is grateful to the Third World Academy of Science (TWAS)-UNESCO and CNPq for providing financial support. The authors are grateful to Núcleo de catálise da COPPE/UFRJ for XRD analysis. The authors are grateful to LNLS, Brazil, for WAXS/SAXS (D11A-SAXS1#5324/06; #6597/07; and #7086/08) analysis.

References

1. Somani, P.; Mandel, A. B.; Radhakkrishnan, S. R. Acta Mater 2000, 48, 2859.
2. Gurunathan, K.; Vadivel Murugan, A.; Marimuthu, P.; Mulik, U. P.; Amalnerrkar, D. P. Mater Chem Phys 1999, 61, 173.
3. Kanungo, M.; Kumar, A.; Contractor, A. Q. J Electroanal Chem 2002, 528, 46.
4. Lindfors, T.; Ivaska, A. Anal Chim Acta 2001, 437, 171.
5. Avlyanov, J. K.; Dahman, S. ACS Symp Ser 1999, 735, 270.
6. Anand, J.; Palaniappan, S.; Sathyanarayana, D. N. Prog Polym Sci 1998, 23, 993.
7. Del Rio, R.; Zagal, J. H.; de, G.; Andrade, T.; Biaggio, S. R. J Appl Electrochem 1999, 29, 759.
8. Wampler, W. A.; Rajeshwara, K.; Pethe, R. G.; Hyer, R. C.; Sharma, S. C. J Mater Res 1996, 10, 1811.
9. Luo, K.; Guo, X. M.; Shi, N. L.; Sun, C. Synth Met 2005, 151, 293.
10. Wu, G.; Li, L.; Li, J. H.; Xu, B. Q. Carbon 2005, 43, 2579.
11. Souza, F. G., Jr.; Sirelli, L.; Michel, R. C.; Soares, B. G.; Herbst, M. H. J Appl Polym Sci 2006, 102, 535.
12. Bourdo, S. E.; Viswanathan, T. Carbon 2005, 43, 2983.
13. Ghanbari, K.; Mousavi, M. F.; Shamsipur, M.; Karami, H. J Power Sources 2007, 170, 513.
14. Sathiyanarayanan, S.; Azim, S. S.; Venkatachari, G. Electrochim Acta 2007, 52, 2068.
15. Wu, T. M.; Lin, Y. W. Polymer 2006, 47, 3576.
16. Jeevananda, T.; Siddaramaiah; Kim, N. H.; Heo, S.-B.; Lee, J. H. Polym Adv Technol 2008, 19, 1754.
17. Jeevananda, T.; Siddaramaiah; Lee, J.-H.; Samir, O. M.; Somashekar, R. J Appl Polym Sci 2008, 109, 200.
18. Darren, A. M.; Trisha, H. Synth Met 2006, 156, 497.
19. Khomenko, V.; Frackowiak, E.; Beguin, F. Electrochim Acta 2005, 50, 2499.
20. Sotzing, G. A.; Phend, J. N.; Grubbs, R. H.; Lewis, N. S. Chem Mater 2000, 12, 593.
21. Sengupta, P. K.; Dan, A.; Mondal, T. Proceedings of the International Conference on Rubbers; Calcutta, India, 1997; p 109.
22. Kan, J. Q.; Li, X.; Li, Y. F. Bull Electrochem 2002, 18, 477.
23. Fraser, R. D. B.; Mac Rae, T. P. Conformation in Fibrous Proteins; Academic press, New York and London, 1973; p 385.
24. Girotto, E. M.; Santos, I. A. Química Nova 2002, 25, 639.
25. Hoseman, R.; Bagchi, S. N. Direct Analysis of Diffraction by Matter; North-Holland Publishing Co.: Amsterdam, North Holland, 1962.
26. Hall, I. H.; Booth, C.; Prince, C. Comprehensive Polymer Science; Pergmon Press: Oxford, UK, 1989; Vol. 1, p 669.
27. Hall, I. H.; Mahamood, E. A.; Carr, P. D.; Geng, Y. Colloid Polym Sci 1987, 265, 383.
28. Du, X. S.; Xiao, M.; Meng, Y. Z. Eur Polym J 2004, 40, 1489.
29. Lux, F. Polymer 1994, 35, 2915.
30. Pouget, J. P.; Josefowicz, M. E.; Epstein, A. J.; Tang, X.; Mac Diarmid, A. G. Macromolecules 1991, 24, 779.
31. Zilberman, M.; Titelman, G. I.; Siegmann, A. J Appl Polym Sci 1997, 66, 243.